



HAL
open science

Determination of free metal ion concentrations with AGNES in low ionic strength media

D. Aguilar, Corinne Parat, J. Galceran, E. Companys, J. Puy, Laurent
Authier, Martine Potin-Gautier

► **To cite this version:**

D. Aguilar, Corinne Parat, J. Galceran, E. Companys, J. Puy, et al.. Determination of free metal ion concentrations with AGNES in low ionic strength media. *Journal of Electroanalytical Chemistry*, 2013, 689, pp.276-283. 10.1016/j.jelechem.2012.11.010 . hal-01444582

HAL Id: hal-01444582

<https://hal.science/hal-01444582>

Submitted on 14 Mar 2018

HAL is a multi-disciplinary open access archive for the deposit and dissemination of scientific research documents, whether they are published or not. The documents may come from teaching and research institutions in France or abroad, or from public or private research centers.

L'archive ouverte pluridisciplinaire **HAL**, est destinée au dépôt et à la diffusion de documents scientifiques de niveau recherche, publiés ou non, émanant des établissements d'enseignement et de recherche français ou étrangers, des laboratoires publics ou privés.

1 Determination of free metal ion concentrations 2 with AGNES in low ionic strength media

3 *D. Aguilar^a, C. Parat^b, J. Galceran^{a*}, E. Company^a, J. Puy^a, L. Authier^b and M. Potin-*
4 *Gautier^b*

5 ^aDepartament de Química. Universitat de Lleida, Rovira Roure 191, 25198 Lleida,
6 Spain

7 ^bUniversité de Pau et des Pays de l'Adour, L.C.A.B.I.E., UMR 5254, IPREM, Av. P.
8 Angot, 64053 Pau Cedex 9, France

9 *corresponding author. E-mail address: galceran@quimica.udl.cat. Tel.:+34-973-70-28-
10 26; fax:+34-973-23-82-64

11 12 **Abstract**

13 The determination of free metal ion concentrations of heavy metals, like Zn²⁺ or Cd²⁺,
14 with AGNES (Absence of Gradients and Nernstian Equilibrium Stripping) requires an
15 adequate selection of parameters such as deposition potential (linked to the gain,
16 $[M^0]/[M^{2+}]$) and deposition time. In systems with low ionic strength, the peak potential
17 of the Differential Pulse Polarogram (DPP) measured with low supporting electrolyte is
18 not always suitable for the computation of the gain with existing expressions. The
19 application of AGNES with a constant potential (regardless of the ionic strength)
20 provides a direct measurement of the metal ion activity. When working with low ionic
21 strength solutions, the selection of appropriate instrumentation is important to avoid
22 changes in liquid junction potentials or leakages from the employed electrodes. The
23 deposition times (for a given gain) have not been found to be greatly affected by the
24 probed ionic strengths when working with just metal. A new strategy for the practical

25 implementation of AGNES to measure free metal ion concentrations in samples with
26 low KNO_3 or $\text{Ca}(\text{NO}_3)_2$ concentrations consists in the computation of the deposition
27 potential (to reach a certain gain) from the DPP peak potential at a sufficiently high
28 ionic strength using a new expression. A speciation experiment with Zn^{2+} and Glycine
29 at pHs between 4 and 7.5, where $[\text{KNO}_3]=0.001$ M, shows that this methodology works
30 well and also proves that it is possible to perform AGNES in systems with very low
31 ionic strength.

32

33 **Keywords:** low ionic strength, electrolyte, free metal concentration, AGNES.

34

35 **1. Introduction**

36 The knowledge of the free ion concentration of heavy metals such as Zn, Cd, Pb or Cu
37 is very important for understanding the role and fate of nutrient and pollutant elements
38 in natural waters [1]. Indeed, the Free Ion Activity Model [2] or the Biotic Ligand
39 Model [3] highlight the free metal concentration as more relevant than the total
40 concentration which can be determined with well established techniques.

41 Few methods exist for the free metal ion determination, for instance, ion selective
42 electrodes (ISEs) [4], Donnan Membrane Technique (DMT) [5], Complexing gel
43 Integrated microelectrode (CGIME) [6], Permeation liquid membrane (PLM) [7], etc. In
44 recent years, AGNES (Absence of Gradients and Nernstian Equilibrium Stripping) has
45 proved to be a successful electroanalytical technique to measure free metal
46 concentrations [8, 9]. Some of its advantages are the relatively short time for a
47 measurement and the easy interpretation of the results [8, 9]. AGNES has been
48 implemented with a wide range of electrodes like Hanging Mercury Drop Electrode
49 (HMDE), Ir-Hg microelectrode [10], Mercury Thin Film in Rotating Disk Electrode

50 [11] or Screen Printed Electrode (SPE) [12] and has been applied to the determination
51 of Zn^{2+} in samples from seawater [13], relatively polluted river waters [14, 15], wine
52 [16] and the dissolution of ZnO nanoparticles [17] and of Cd quantum dots [18].

53 The study of solutions, like pristine natural waters or synthetic preparations, with very
54 low supporting electrolyte concentrations can become a challenge since voltammetric
55 and potentiometric measurements can depart significantly from the traditional
56 experiments with higher ionic strengths [19, 20]. In solutions with large amounts of
57 supporting electrolyte, the electric field associated with the potential drop is confined to
58 a narrow interfacial region, and the transport of ions from or to the electrode occurs only
59 by diffusion (electroactive species migration is suppressed, see page 441 in [21]).
60 Furthermore, a high ionic strength also provides a constant activity coefficient. On the
61 other hand, insufficient excess of supporting electrolyte leads to solutions of very high
62 resistance, i.e. the potential drop is not located just at the interphase, but extends into the
63 solution phase leading to migrational effects [20, 22-24]. Additional potential drops at
64 the liquid junction also arise. In solutions with low electrolyte concentration, one option
65 to avoid these problems is the addition of an ionic electrolyte to increase the solution
66 ionic strength, but it might impact on the investigated system by introducing additional
67 chemical equilibria, changes in the activity coefficients and/or contamination.

68 In a previous work [15], we have determined the free Zn concentration of a natural
69 water with relatively low ionic strength where a standard AGNES procedure proved
70 sufficient. However, the lowest examined ionic strength in that work (0.004 mol L^{-1}) is
71 higher than the ones needed for pristine natural waters or some synthetic solutions. An
72 improvement of the accuracy would also be convenient. In the present work, we aim at
73 a comprehensive physicochemical study on the impact of ionic strength on AGNES
74 analytical signal, in order to develop a general methodology for determining the free

75 concentration of heavy metals, like Zn^{2+} or Cd^{2+} , in solutions with ionic strengths
76 between 0.001 and 0.1 mol L^{-1} without the addition of any extra supporting electrolyte.
77 This study includes the impact of different supporting electrolytes, such as KNO_3 and
78 $Ca(NO_3)_2$, to the free metal measurements and the finding of suitable experimental
79 settings for these kinds of samples.

80 **2. Materials and Methods**

81 **2.1 Procedures**

82 AGNES consists of two conceptual stages [8, 9]. In the first one, a deposition potential
83 E_1 is applied, for a time t_1 , to reduce the analyte metal until a special situation of
84 Nernstian equilibrium, with no concentration gradient at each side of the electrode, is
85 reached. We call gain, Y , to the ratio between the reduced metal concentration inside the
86 amalgam $[M^0]$ and the free metal ion concentration $[M^{2+}]$. The gain can be computed
87 with Nernst law as:

$$88 \quad Y = \frac{[M^0]}{[M^{2+}]} = \frac{\gamma_{M^{2+}}}{\gamma_{M^0}} \exp\left[-\frac{nF}{RT}(E_1 - E^0)\right] = \exp\left[-\frac{nF}{RT}(E_1 - E^{0'})\right] \quad (1)$$

89 where n is the number of electrons involved in the faradaic process, γ_i is the activity
90 coefficient of species i (computed, when necessary, with Davies equation), F is the
91 Faraday constant, R is the gas constant, T is the temperature, E^0 is the standard redox
92 potential and $E^{0'}$ is the standard formal potential.

93 To avoid the explicit finding of E^0 or $E^{0'}$, the potential corresponding to a given Y has,
94 up to date, been determined from the peak potential of a differential pulse polarogram
95 (DPP)[8]:

$$96 \quad Y = \sqrt{\frac{D_M}{D_{M^0}}} \exp\left[-\frac{nF}{RT}\left(E_1 - E_{\text{peak}} - \frac{\Delta E}{2}\right)\right] \quad (2)$$

97 where E_{peak} refers to the potential of the maximum obtained in a typical I vs E DPP plot,
98 D_{M} ($7.03 \times 10^{-10} \text{ m}^2\text{s}^{-1}$ for Zn and $7.30 \times 10^{-10} \text{ m}^2\text{s}^{-1}$ for Cd) is the diffusion coefficient for
99 the free metal ion in solution, D_{M^0} ($1.81 \times 10^{-9} \text{ m}^2\text{s}^{-1}$ for Zn and $1.60 \times 10^{-9} \text{ m}^2\text{s}^{-1}$ for Cd) is
100 the diffusion coefficients for the reduced metal inside the amalgam (the changes of the
101 diffusion coefficients with the ionic strength have been considered negligible), and ΔE
102 is the modulation amplitude of the DPP experiment.

103 During the second stage of AGNES, the accumulated metal is reoxidated and
104 quantified.

105 In the present work, we have applied a constant potential pulse E_2 under diffusion
106 limited conditions, taking the charge Q as analytical response to avoid the anomalous
107 stripping behaviours described for low ionic strengths in [15, 25] which could affect the
108 intensity current.

109 From the combination of Nernst and Faraday laws, the charge can be correlated to the
110 free metal concentration

$$111 \quad Q = Y\eta_Q [M^{2+}] \quad (3)$$

112 where η_Q is a proportionality factor that can be obtained from a calibration plot.

113 In all cases, it is important to note that there is no need to exactly know the gain Y
114 prescribed in the first AGNES stage, because the off-set in the measurement is cancelled
115 out by the off-set in the calibration in the same medium. However, a good estimation of
116 the Y helps in searching for adequate deposition times and to check the proportionality
117 factor (η_Q) found in a new calibration with previously reported values [12, 26].

118

119 **2.2 Equipment and Reagents**

120 Potassium nitrate and calcium nitrate solutions were used as the inert supporting
121 electrolytes to obtain ionic strengths between 0.001 and 0.1 mol L⁻¹ and were prepared

122 from solid KNO_3 (Fluka, TraceSelect) and $\text{Ca}(\text{NO}_3)_2$ (Merck, Suprapur). Glycine was
123 obtained from Fluka (ReagentPlus, $\geq 99\%$). Nitric acid (69-70%, Baker Instra-Analysed
124 for trace metal analysis), sodium hydroxide (Baker Analysed), hydrochloric acid (Baker
125 Instra-Analysed for trace metal analysis) were obtained from J.T. Baker. The stock
126 solutions of Zn and Cd were obtained from Merck (analytical grade).

127 Ultrapure water (Milli-Q plus 185 System, Millipore) of $18 \text{ M}\Omega \text{ cm}$ resistivity was
128 employed in all the experiments. Purified water-saturated nitrogen N_2 was used for
129 deaeration of solutions.

130 Voltammetric measurements were carried out using an Eco Chemie Autolab PGSTAT
131 10 potentiostat attached to a Metrohm 663 VA Stand and to a computer by means of the
132 GPES 4.9 (Eco Chemie) software package. The working electrode was a Metrohm
133 multimode mercury drop electrode with the largest drop in our stand (drop 3)-if we
134 perform DPPs- or the smallest drop in our stand (drop 1) -if we perform AGNES-,
135 which corresponds, according to the catalogue, to a radius around $r_0=4.23 \times 10^{-4}$ or
136 1.41×10^{-4} m, respectively. DPP parameters used in this work have been: modulation
137 time 10 ms, interval time 1 s, step potential 0.00105 V and modulation amplitude
138 0.04995 V. The auxiliary electrode was a glassy carbon electrode and the reference
139 electrodes were: i) $\text{Ag} | \text{AgCl} | \text{KCl}$ (3 mol L^{-1}) encased in a 1 or 0.1 mol L^{-1} KNO_3
140 jacket (ref. 6.0726.100 from Metrohm) which, for simplicity, is labelled here as “glass
141 electrode”; ii) $\text{Ag} | \text{AgCl} | \text{KCl}$ saturated 3% LGL agarose gel described in [27]; iii)
142 Calomel with a KNO_3 0.1 mol L^{-1} jacket (ref. 421 from Radiometer Analytical); iv) $\text{Ag} |$
143 $\text{AgCl} | \text{KCl}$ saturated, without salt bridge, from Origalys Electrochem (ref.
144 E11.OGL.014). During the execution of all the experiments, conductivity measurements
145 were carried out with an Orion 0103010MD probe, from Thermo Scientific, to check
146 the attainment of the different studied ionic strengths. With the $\text{Ag} | \text{AgCl} | \text{KCl}$ (3 mol

147 L⁻¹), Calomel or Ag | AgCl | KCl (agarose gel) electrodes, we observed small increases
148 of the conductivity with time (15-20 μ S/ hour), during the study of a unique ionic
149 strength, due to a leakage from the reference electrode. The impact of these leakages in
150 the results was so small that they could be considered negligible. With the Ag | AgCl |
151 KCl saturated from Orignalys, the sample conductivity increased around 90-120 μ S/hour,
152 which can be especially problematic when working with very low ionic strengths (in
153 one hour, the ionic strength of a $\mu=0.001$ mol L⁻¹ sample could double).

154 A glass combined electrode (Orion 9103) was attached to an Orion Research 720A
155 ionanalyzer and introduced sporadically in the cell to control de pH. A glass jacketed
156 cell provided by Metrohm, thermostated at 25.0°C, was used in all the experiments.

157

158 **3. Results and discussion**

159 **3.1 The use of Y computed from the E_{peak} of a DPP at the same ionic** 160 **strength of the sample medium**

161 Up to date, the standard application of AGNES in a given medium has consisted in the
162 determination of the deposition (and stripping) potentials by using eqn. (2), where the
163 DPP peak potential E_{peak} was determined in the same medium or as close as possible to
164 it. So, according to this classical methodology, to apply AGNES at low ionic strength,
165 one should start by running a DPP in these conditions.

166 The influence of the supporting electrolyte concentration (KNO₃ or Ca(NO₃)₂ in the
167 range 0.001 to 0.1 mol L⁻¹) on the potential peak of a DPP has been evaluated in
168 different solutions with $c_{\text{T,M}}=7.5 \times 10^{-6}$ mol L⁻¹ of Zn²⁺ or Cd²⁺. The jacket/bridge of the
169 Ag/AgCl reference electrode used was filled with a KNO₃ 0.1 mol L⁻¹ solution. The
170 experiments were carried out with a fixed pH at 5.5 adjusted with the addition of acid or
171 base and the ionic strength, in all the performed experiments, has been computed with

172 Visual Minteq [28]. Figure 1 shows how E_{peak} changes with the ionic strength for a
173 Zn^{2+} sample in KNO_3 : it increases (i.e. moves towards less negative values) sharply at
174 very low ionic strengths ($0.001\text{-}0.005 \text{ mol L}^{-1}$) and, after reaching a maximum, the
175 potential smoothly decays for higher KNO_3 concentrations ($0.005\text{-}0.1 \text{ mol L}^{-1}$). The
176 same kind of results were also obtained with Zn^{2+} in $\text{Ca}(\text{NO}_3)_2$ as supporting electrolyte
177 (with 0.1 or 1 mol L^{-1} KNO_3 in the salt bridge; data not shown).

178 On the other hand, measurements of Cd^{2+} in both KNO_3 or $\text{Ca}(\text{NO}_3)_2$ (Figure SI-1 in the
179 Supporting Information) were also carried out and we observed a general similar trend:
180 the E_{peak} slightly increases for low electrolyte concentrations between 0.001 and 0.007
181 mol L^{-1} and decreases (more negative values) from 0.007 mol L^{-1} to higher ionic
182 strengths.

183 The slow decrease of E_{peak} with sufficiently high ionic strength can be explained from
184 the changes in the activity coefficients, see eqns. (7.3.20) and (2.1.45) in [29] and eqn.
185 (5), below. The fast rising behaviour of the DPP peak potential at very low ionic
186 strengths, with Zn^{2+} and Cd^{2+} in both KNO_3 or $\text{Ca}(\text{NO}_3)_2$, could be partially due to
187 migrational effects and, especially in the Zn^{2+} case, the steep variation could, perhaps,
188 also be associated to the irreversibility of the couple $\text{Zn}^0/\text{Zn}^{2+}$ [30, 31]. For Zn^{2+} ,
189 analogous results were obtained with other reference electrodes such as Calomel or $\text{Ag} |$
190 $\text{AgCl} | \text{KCl}$ saturated from Orignalys (Figure SI-2). However, given that the anomalous
191 behaviour with Cd^{2+} has not been observed with Orignalys reference electrode (see
192 Figure SI-3), its most likely reason could be a sluggish response in the salt bridge
193 junction. Unfortunately, Orignalys has a large leakage (see section 2.2.) and it is not
194 suitable for long experiments with AGNES at low ionic strength.

195 Following the standard methodology of computing E_1 from the peak potentials of DPP
196 in the same medium (i.e. eqn. (2)), AGNES has been run with HMDE at different ionic

197 strengths ($\mu=0.001, 0.002, 0.005, 0.01$ and 0.1 mol L^{-1}). The study has been performed
198 with a deaerated $c_{\text{T,Zn}} = 2.5 \times 10^{-6} \text{ mol L}^{-1}$ sample in KNO_3 , since, in that medium, Zn^{2+} is
199 the metal that presents a greater E_{peak} change at low electrolyte concentrations (compare
200 Figure 1 with Figure SI-1). Figure 2 shows the accumulated charge, Q , with increasing
201 deposition times t_1 , between 100 and 3000 s, aiming at a gain of $Y=50$. These Q vs t_1
202 trajectories exhibited the typical shape: a fast initial increase followed by an
203 asymptotical tendency towards the stabilized AGNES equilibrium value. Previous
204 published results [8, 9, 32], indicated that, with HMDE and vigorous stirring, a
205 deposition time around seven times the gain is enough for reaching AGNES equilibrium
206 in samples with supporting electrolyte 0.05 mol L^{-1} and higher. However, we see now
207 in Figure 2, that for very low ionic strengths, the t_1 -values needed to reach equilibrium
208 are much longer than those suggested with the rule $t_1=7Y$: e.g. $t_1=2500$ s was needed for
209 $Y=50$ when $\mu=0.001 \text{ mol L}^{-1}$. This is a warning that the gain aimed in these samples
210 might be higher than the supposedly prescribed one ($Y=50$).

211 In order to estimate which has been the real gain applied in all the different analysed
212 samples, we can apply Faraday law [12, 26] to find the “real” or “experimental from
213 charge” gain Y_Q

$$214 \quad Y_Q = \frac{Q}{nFV_{\text{Hg}} [\text{Zn}^{2+}]} \quad (4)$$

215 where Q is the experimental accumulated charge up to reach Nernstian equilibrium, V_{Hg}
216 is the electrode mercury volume and $[\text{Zn}^{2+}]$ is the free analyte concentration (which in
217 this case can be computed with Visual Minteq).

218 Red markers \times in Figure 3 show that the gain really applied (Y_Q) was not constant at the
219 different ionic strengths, when the deposition potential was computed with eqn. (2) and
220 the potential peaks obtained from the DPP experiment. The obtained gains follow an

221 opposite trend to the DPP peak potentials (compare with Figure 1): the more negative
222 the measured DPP potential, the more negative the computed E_1 and the higher the
223 resulting real gain. As the electrolyte concentration increases (near 0.1 mol L^{-1}), the real
224 gain begins to stabilize around the value of 50, which is the gain initially intended for
225 all the samples. Comparing Figures 2 and 3, the deposition times t_1 needed to reach
226 equilibrium follow the aforementioned AGNES rule $t_1=7Y$ for all the ionic strengths
227 studied between 0.001 and 0.1 mol L^{-1} (i.e. using the real gain). This result contrasts
228 with the possibly expected reduction in the deposition times to reach a certain gain for
229 low supporting electrolyte concentrations due to a greater contribution of migration
230 between the working and reference electrodes (section 4.3, p140 in [29]).
231 Thus, the application of a deposition potential E_1 computed from its corresponding
232 E_{peak} , at low ionic strengths, does not produce the intended gain and could lead to an
233 underestimation of the achieved charge and, therefore, of the free metal concentration if
234 the usual deposition times (rule $t_1=7Y$) was followed blindly (i.e. without checking for
235 the attainment of the sought equilibrium). In experiments in Figure 2, apart from the
236 inadequacy of the deposition times, the equilibrium charges reached –assuming $Y=50$ –
237 lead to η_Q values ($1.1 \times 10^{-3} - 1.7 \times 10^{-2} \text{ C/M}$) at odds with the standard values for
238 HMDE (around $2.0 \times 10^{-3} \text{ C/M}$ [12]) while values in the range $2.0 - 2.3 \times 10^{-3} \text{ C/M}$ are
239 obtained with the measured gains Y_Q .
240 These anomalous attained gains seem related to an inadequacy of Zn^{2+} DPPs at low
241 ionic strengths. This fact has been corroborated by plotting the E_{peaks} , obtained from the
242 DPPs between $\mu=0.001$ and 0.1 mol L^{-1} , versus the activity coefficient logarithm (ln
243 $\gamma_{\text{M}^{n+}}$). Indeed, combining eqn. (1) and (2),

244
$$E_{\text{peak}} = E^0 + \frac{RT}{nF} \ln \sqrt{\frac{D_{\text{R}}}{D_{\text{O}}}} - \frac{\Delta E}{2} + \frac{RT}{nF} \ln \frac{\gamma_{\text{M}^{n+}}}{\gamma_{\text{M}^{n0}}} \quad (5)$$

245 which prescribes that the relationship between E_{peak} and $\ln \gamma_{M^{n+}}$ (considering
246 $[M^0]=\{M^0\}$, where $\{M^0\}$ is the metal activity) has to be lineal with a slope close to
247 $RT/(nF)\approx 0.013$ V). Figure 4, shows the plot corresponding to a $c_{T,Zn} = 7.5\times 10^{-6}$ mol L⁻¹
248 in KNO₃ sample (blue squares) where the expected linear behaviour with a slope close
249 to 0.013 V is clearly found at least for ionic strengths equal or higher than 0.01 mol L⁻¹.
250 This indicates that DPP at low supporting electrolyte concentrations cannot be safely
251 used for determining AGNES gains. Similar results have been found for Cd and KNO₃
252 or Ca(NO₃)₂ as the background electrolyte (see Figure 4 red circles). When working
253 with the Ca(NO₃)₂ electrolyte, we suggest the use of a reference electrode with a jacket
254 filled with KNO₃ 1 M, since DPPs are more reproducible and liquid junction potentials
255 are minimized as observed in the attainment of more accurate Nernstian slopes in the
256 E_{peak} vs. $\ln \gamma_{M^{n+}}$ plots. Our current interpretation of these results is that eqn. (2) was
257 derived taking into account diffusion as the sole transport phenomenon, neglecting
258 migration and the possible sluggishness of the reference electrode. We can conclude
259 that eqn. (2) might be inaccurate for ionic strengths below 0.01 mol L⁻¹ when working
260 with Zn²⁺ or Cd²⁺ in KNO₃ and Ca(NO₃)₂.

261

262 **3.2 The application of a fixed E_1 at all ionic strengths**

263 Since, at low ionic strengths, the deposition potentials cannot be computed with eqn.
264 (2), we proceed to study how AGNES behaves when a unique fixed deposition potential
265 (E_1) is applied at different ionic strengths in an aqueous sample. This study will allow
266 us to establish under which conditions AGNES principles can be applied.

267 **3.2.1 Theory for a fixed deposition potential**

268 **3.2.1.1 Determining the metal ion activity**

269 Faraday law can be written as

270 $Q = nFV_{\text{Hg}} [M^0]$ (6)

271 Assuming $\gamma_{M^0} = 1$, Nernst law (1) can be recast as

272 $\frac{Q}{\{M^{2+}\}} = nFV_{\text{Hg}} \exp\left[-\frac{nF}{RT}(E_1 - E^0)\right] \equiv f$ (7)

273 where we have introduced a new proportionality factor f . So, when applying a fixed
274 deposition potential, the accumulated charge in AGNES equilibrium is directly
275 proportional to the analyte activity $\{M^{2+}\}$ regardless of the ionic strength of the
276 medium.

277 One possible way of implementing AGNES could be to measure the activity with a
278 fixed potential and then, via the estimation of activity coefficients in the medium,
279 compute the analyte concentration. However, in this work, we aim at a direct
280 determination of the free concentration and we will use eqn. (7) only to confirm the
281 range of validity of the obtained results within the current interpretative framework.

282

283 **3.2.1.2 Relationship between formal potential and activity coefficient**

284

285 When changing the ionic strength, the formal potential and the standard redox potential
286 are related through (see eqn. 2.1.45 in [29])

287 $E^{0'} = E^0 + \frac{RT}{nF} \ln\left(\frac{\gamma_{M^{2+}}}{\gamma_{M^0}}\right)$ (8)

288 Assuming $\gamma_{M^0} = 1$, one expects a linear relationship between $E^{0'}$ and the logarithm of
289 the activity coefficient with a slope equivalent to $RT/(nF) \approx 0.013$ V at approximately
290 25°C. This property will be used next to establish conditions for an adequate AGNES
291 implementation.

292 In practice, we can compute $E^{0'}$ from an AGNES measurement: combining Nernst law
293 (1) with Faraday law (6)

294
$$\frac{Q/(nFV_{\text{Hg}})}{[M^{2+}]} = \exp\left[-\frac{nF}{RT}(E_1 - E^{o'})\right]$$
 (9)

295 so that

296
$$E^{o'} = E_1 + \frac{RT}{nF} \ln Y_Q$$
 (10)

297 where Y_Q is the experimental gain computed with eqn. (4).

298

299 3.2.2 Results with KNO_3 as supporting electrolyte

300 Experiments at fixed deposition potential were carried out in solutions containing

301 $c_{\text{T,M}}=2.5 \times 10^{-6} \text{ mol L}^{-1}$ of Zn^{2+} or Cd^{2+} , μ between 0.001 and 0.1 mol L^{-1} , at $\text{pH}=5.5$ and

302 25.0°C . A KNO_3 0.1 mol L^{-1} salt bridge was used in the reference electrode. AGNES

303 stripping stage consisted in the application of a fixed potential under diffusion limited

304 conditions (for reoxidation), while E_1 (regardless of the ionic strength of the solution)

305 has been computed using eqn. (2) and the E_{peak} corresponding to the highest electrolyte

306 concentration studied ($\mu=0.1 \text{ mol L}^{-1}$), aiming at a gain $Y=50$.

307 In the studied samples, we have observed that the deposition time needed to reach

308 Nernstian equilibrium in HMDE measurements is around 1000 s for samples with ionic

309 strengths between 0.001 and 0.01 mol L^{-1} , indicating, again, that the experimental gain

310 applied in these solutions (which can be estimated with eqn. (4)) is not the intended one

311 ($Y=50$) (see the Zn^{2+} case in Figure SI-4). On the other hand, for the KNO_3 0.1 mol L^{-1}

312 sample, the computed experimental gain and the deposition time needed to reach

313 equilibrium (around 400 s) are consistent with $Y=50$ (Figure SI-4).

314 With eqn. (10), we computed the corresponding $E^{o'}$ for the samples with the different

315 ionic strengths tested. All the obtained $E^{o'}$, for solutions with Zn^{2+} or Cd^{2+} in KNO_3 ,

316 follow Nernst law, since their representation versus the logarithm of the activity

317 coefficient is linear with the expected slope $RT/nF \approx 0.013$ V (see blue squares in Figure
318 5) according to eqn. (8).

319 These results indicate that, under the aforementioned conditions, AGNES can be
320 applied satisfactorily in solutions with very low supporting electrolyte concentrations.
321 For the practical computations, though, one must take into account the change in the
322 activity coefficients (e.g. via Davies equation) at each of the ionic strengths tested.

323 The same conclusion can be drawn from eqn. 7. It predicts the collapse of curves
324 $Q/\{Zn^{2+}\}$ vs t_1 , seen in Figure 6 for sufficiently long deposition times (i.e. once AGNES
325 conditions are reached) in all the studied samples. Very similar results were also
326 obtained with Cd^{2+} (Figure SI-5, blue squares).

327 This property paves the way for future work where the proportionality factor f in
328 AGNES could be calibrated in activities at a fixed potential at a (comfortable) given
329 ionic strength, and, then, the measured charge in the sample is converted into metal ion
330 activity.

331 3.2.3 Results with $Ca(NO_3)_2$ as supporting electrolyte

332 On the other hand, when $Ca(NO_3)_2$ is the supporting electrolyte, we observe the same
333 trends as with KNO_3 : applying a fixed E_1 in samples with different ionic strengths
334 between 0.001 and 0.1 mol L⁻¹, does not produce a fixed gain, especially at low ionic
335 strengths.

336 However, when representing $E^{0'}$, computed at each ionic strength using eqn. (10),
337 versus the activity coefficient logarithm, we observe that the linear behaviour, with the
338 expected $RT/(nF)$ slope, is only fulfilled for ionic strengths lower than 0.01 M (see
339 Figure 5, red circles). In the same way, the f factor, eqn. (7), for these $Ca(NO_3)_2$
340 solutions, is only constant for $\mu < 0.01$ M (Figure SI-5, red circles). We did not observe
341 any improvement in the results when working with other salt bridges concentrations

342 (KNO₃ 0.1 or 3 mol L⁻¹) or other reference electrodes like Calomel or the gel salt bridge
343 described in [27]. However, the Ag/AgCl reference electrode saturated with KCl from
344 Orignalys Electrochem showed a Nernstian linearity for all the ionic strength range
345 studied $\mu=0.001 - 0.14$ mol L⁻¹ (Figure SI-6). Compared with the glass reference one,
346 the applicability range of this electrode would be larger if it did not present a large
347 leakage (see Section 2.2.).

348 The reason for the deviation of E° from the expected linearity when using Ca(NO₃)₂ as
349 supporting electrolyte and $\mu>0.01$ M (see Figure 5, red bullets) is unclear to us. We
350 discard problems derived from a bad estimation of the activity coefficients, since good
351 results were observed in the same range of ionic strengths when measuring DPP peak
352 potentials with the same background electrolyte (Figure 4, red circles). A similar
353 reasoning could discard liquid junction potential, unless the discrepancy in behaviour
354 with Ca(NO₃)₂ at $\mu>0.01$ M in Figures 4 and 5 was due to the different time scale
355 (and/or the stirring) of DPP and AGNES measurements (e.g. via a different impact of
356 the uncompensated resistance at low ionic strength in both techniques). We also discard
357 effects of ion pairing association between Ca and nitrate ions, because of the observed
358 linear increase of conductivity with increasing concentration of Ca(NO₃)₂.

359 We conclude that the existing methodologies of AGNES can be applied, when using
360 Ca(NO₃)₂ below 0.01 M as supporting electrolyte. For instance, this should not be a
361 problem when studying a freshwater where the total concentration of Ca is usually
362 below 0.01 M.

363

364 **3.3 The computation of the gain for any ionic strength from a DPP** 365 **peak at high enough ionic strength**

366 In previous sections, we have explained how, in some cases, E_{peaks} from DPPs at low
367 ionic strengths ($\mu<0.01$ M) are unsuitable for the gain computation and how AGNES

368 can be applied properly in the low ionic strength range ($\mu \leq 0.01$ M) with Zn^{2+} or Cd^{2+}
369 and KNO_3 or $\text{Ca}(\text{NO}_3)_2$ as supporting electrolytes. Now, we consider whether it is
370 possible to use the peak potential of a DPP run at a sufficiently high ionic strength
371 (where the DPP follows the behaviour prescribed by eqn. (5), say $\mu \geq 0.01$ as seen in
372 Figure 4), in order to compute the deposition potential for a certain gain in an AGNES
373 experiment at any other ionic strength.

374 We can equate eqn. (1) for the desired gain at a sufficiently high ionic strength with eqn.
375 (1) for the same gain at another supporting electrolyte concentration:

$$376 \frac{\gamma_{\text{M}^{2+}}}{\gamma_{\text{M}^0}} \exp \left[-\frac{nF}{RT} (E_1 - E^0) \right] = \frac{\gamma_{\text{M}^{2+}}^{\mu \geq 0.01}}{\gamma_{\text{M}^0}^{\mu \geq 0.01}} \exp \left[-\frac{nF}{RT} (E_1^{\mu \geq 0.01} - E^0) \right]$$

377 (11)

378 Combining eqn. (11) with eqn. (2), we obtain an expression that allows the computation
379 of E_1 at any ionic strength, to reach a certain Y , just using the DPP of a solution with
380 $\mu \geq 0.01$ and a correction involving the activity coefficients:

$$381 E_1 = E_{\text{peak}}^{\mu \geq 0.01} + \frac{\Delta E}{2} + \frac{RT}{nF} \ln \left(\frac{\gamma_{\text{M}}}{\gamma_{\text{M}}^{\mu \geq 0.01} Y} \sqrt{\frac{D_{\text{M}}}{D_{\text{M}^0}}} \right)$$

382 (12)

383 To illustrate this method, eqn. (12) has been used to compute the corresponding
384 deposition potential in AGNES measurements in order to reach a certain gain.
385 Trajectories Q vs t_1 have been studied by applying AGNES to a deareated
386 $c_{\text{T,Zn}} = 2.5 \times 10^{-6}$ mol L⁻¹ solution with $\mu = 0.001, 0.005, 0.01$ and 0.1 mol L⁻¹ provided by
387 KNO_3 . The corresponding deposition potentials E_1 , aiming to $Y=50$, have been
388 computed using eqn. (12) with $E_{\text{peak}}^{\mu=0.1}$ ($\mu = 0.1$ has been selected to be on the safe side,
389 but –according to the study in section 3.2– any E_{peak} for μ between 0.01 and 0.1 mol L⁻¹
390 should be also valid). Figure 7 shows the representation of $Q/[\text{Zn}^{2+}]$ in front of t_1 . The
391 curves for the different electrolyte concentrations tested practically collapse indicating
that the achieved accumulation is the same for all the samples at each deposition time.

392 Moreover, the accumulated charge reaches AGNES conditions for a t_1 around 350 s
393 (Figure 7), which is the suggested time for a gain $Y=50$.

394 On the other hand, with the deposition potentials E_1 values from section 3.1, (obtained
395 from DPPs at different ionic strengths), we can calculate, with eqn. (12), the theoretical
396 gain applied in the AGNES experiment (blue circles in Figure 3). These theoretical Y
397 values compare very well with the experimental ones (Y_Q , \times marker in Figure 3)
398 obtained with eqn. (4).

399

400 **3.4 Practical strategies**

401 We discuss here a possible strategy to determine the free metal ion concentration in a
402 sample, synthetic or natural, at known low ionic strength (i.e. we assume that we can
403 estimate or compute the value of the activity coefficient of the metal ion in the sample;
404 e.g. when the ionic strength of the sample could be estimated from its conductivity
405 [33]).

406 At very low ionic strengths, we have observed that for Zn or Cd with KNO_3 or
407 $\text{Ca}(\text{NO}_3)_2$ as the background electrolytes, the use of DPP is problematic and could lead
408 to large errors in the deposition potentials or times and, thus, in the equilibrium charge.

409 Therefore, we suggest a general methodology to apply AGNES in low ionic strength
410 samples. First of all, we obtain the DPP peak potential in our experimental setup with a
411 high ionic strength ($\mu \geq 0.01 \text{ mol L}^{-1}$ fixed, for instance, with KNO_3). With this $E_{\text{peak}}^{\mu \geq 0.01}$,
412 we apply eqn. (12) to estimate the corresponding deposition potential E_1 and deposition
413 time t_1 (for both calibration and measurements), at the sample's low ionic strength, to
414 reach any desired gain Y . This estimation is very convenient to have a good guideline of
415 the required deposition time to reach equilibrium and helps avoiding the performance of
416 a full trajectory experiment (similar to the one shown in Figure 2) which is quite long

417 when using HMDE (especially if the Y is rather high). Then, we calibrate our system
418 using solutions of known free metal ion concentrations at the same ionic strength of the
419 sample and assuming the Y previously aimed with eqn. (12). The obtained η_Q value
420 should be similar to those found for high ionic strengths and should be comparable to
421 other published results [12]. Finally, in the sample measurement (e.g. river water),
422 AGNES can be applied using a desired gain (Y) whose corresponding deposition
423 potential can be computed with eqn. (12) and $E_{\text{peak}}^{\mu \geq 0.01}$. With the measured accumulated
424 charge Q_{sample} and the previously found η_Q constant from the calibration, the free
425 concentration of metal $[M^{2+}]$ can be obtained using eqn. (3). Errors in the estimation of
426 the gain Y could appear, but they are not a problem at all, provided that one checks that
427 the used deposition times are enough to reach Nernstian equilibrium. The effect of the
428 uncompensated resistance, arising between the working and the reference electrode due
429 to the low ionic strength of the electrolyte solution, could slightly affect on the
430 determination of the E_{peak} in a DPP measurement and could lead to a small error in the
431 estimation of the gain Y . However, the final error in the determination could be much
432 less than the imprecision in the gain Y , since the error in the gains cancels out between
433 calibration and measurement. This uncompensated resistance does not affect neither to
434 the AGNES deposition stage, since the measured intensity tends to zero once
435 equilibrium is reached, nor to the stripping stage, as we work under diffusion limited
436 conditions (and a small variation of the stripping potential is negligible).

437 To check how reliable are AGNES experiments in low ionic strength samples, we have
438 applied this new strategy to the measurement of the free Zn^{2+} concentration in a
439 solution containing $c_{T,Zn}=3.0 \times 10^{-6}$ mol L⁻¹, glycine 0.01 mol L⁻¹ and $[KNO_3]=9 \times 10^{-4}$
440 mol L⁻¹ at different pHs (4-7.5). The ionic strength in all the performed experiments has
441 been 0.001 mol L⁻¹. The experimental settings have been $E_1=-1.0980$ V (computed

442 using eqn. (12) with $E_{\text{peak}}^{\mu=0.1} = -0.9590$ V and aiming at $Y=50$) during $t_1=350$ s and $E_2=-$
443 0.7534 V, under diffusion limited conditions. The retrieved free Zn^{2+} concentrations at
444 the different pHs studied are in good agreement with the theoretical ones computed with
445 Visual Minteq (Figure 8). This experiment demonstrates how it is possible to perform
446 AGNES measurements in systems with very low supporting electrolyte concentrations.

447

448 **4. Conclusions**

449 In the present work, AGNES technique has been implemented to measure free
450 concentrations of heavy metals (such as Zn^{2+} or Cd^{2+}) in very low ionic strength
451 synthetic systems using both KNO_3 and $\text{Ca}(\text{NO}_3)_2$ as supporting electrolytes. We have
452 observed that the peak potentials of the DPPs performed at μ below 0.01 mol L^{-1} could
453 be not suitable for the computation of the deposition potential E_1 needed to prescribe an
454 intended gain Y when working with Zn^{2+} or Cd^{2+} in both electrolytes. Although the
455 exact knowledge of the applied Y is not strictly necessary (provided that AGNES
456 calibration and measurement use the same E_{peak} , E^0 or $E^{0'}$), the estimation of a good
457 value is very helpful in establishing adequate deposition times t_1 that ensure Nernstian
458 equilibrium and in checking the obtained proportionality factors with those in the
459 literature.

460 The accumulated charges in AGNES, when applying the same fixed deposition
461 potential at different ionic strengths, strongly depend on the supporting electrolyte
462 concentration, due to the changes in the metal ion activity. We have shown that the
463 metal ion activity can be directly measured with AGNES using a constant deposition
464 potential E_1 (see eqn. (7)). The quotient $Q/\{\text{M}^{2+}\}$ appears to be constant in the low ionic
465 strength range ($\mu \leq 0.01 \text{ mol L}^{-1}$), for a fixed E_1 and sufficiently long deposition time for
466 both KNO_3 and $\text{Ca}(\text{NO}_3)_2$ as background electrolytes (see, for example, Figure 6). So,

467 one possible strategy (not developed here) with AGNES consists in first measuring the
468 activity and, then, computing the concentration.

469 For directly measuring the free concentration (see section 3.4) in the range $\mu \leq 0.01$ mol
470 L^{-1} with HMDE, we suggest a new general methodology, for both metals and both
471 supporting electrolytes, consisting in the use of equation (12), which allows estimating
472 the deposition potential at any ionic strength to reach a certain Y , using a proper DPP
473 peak at a high ionic strength ($\mu \geq 0.01$ mol L^{-1}). When working with so low ionic
474 strengths, special care has to be taken to avoid changes in liquid junction potentials or
475 leakages from the used electrodes. In this work, a reference Ag | AgCl encased in a 0.1
476 mol L^{-1} KNO_3 jacket was employed and the aforementioned problems were considered
477 negligible, but a salt bridge solution of 1 mol L^{-1} KNO_3 was specifically appropriate for
478 solutions with $Ca(NO_3)_2$ as background electrolyte. We have not found any relevant
479 impact of ionic strength on the deposition time required for AGNES equilibrium, so the
480 standard rule $t_1 = 7Y$ is applicable at all assayed concentrations of supporting electrolyte
481 (provided that the real Y is used).

482 Eqn. (12), which can be seen as an extension of eqn. (2), represents a step further
483 towards the application of AGNES to systems with low ionic strength. A speciation
484 study in a system containing Zn^{2+} and glycine with $\mu = 0.001$ M, at pHs between 4 and
485 7.5, confirms the validity of the new methodology and the possibility of applying
486 AGNES to solutions with very low supporting electrolyte concentrations.

487

488 **Acknowledgements**

489 The authors acknowledge support of this research from the Communauté
490 d'Agglomération de Pau Pyrénées (CDAPP), from the Spanish *Ministerio de Ciencia e*
491 *Innovación* (CTQ2009-07831 and CTM2009-14612), from the European Community

492 EFA15/08 (PyrMet) and from the *Comissionat d'Universitats i Recerca de la*
493 *Generalitat de Catalunya* (2009SGR00465).

494

495 **Reference List**

496 1. P. G. C. Campbell, in A.Tessier, D.R.Turner (Eds.), *Metal Speciation and*
497 *Bioavailability in Aquatic Systems*, John Wiley & Sons, Chichester (UK), 1995,
498 Ch.2.

499 2. F. M. M. Morel, *Principles and applications of aquatic chemistry*, Wiley, New York,
500 1983.

501 3. P. G. C. Campbell, O. Errecalde, C. Fortin, W. R. Hiriart-Baer, B. Vigneault, *Comp.*
502 *Biochem. Physiol. C*, 133 (2002) 189.

503 4. E. Bakker, E. Pretsch, *Angew. Chem. Int. Edit.*, 46 (2007) 5660.

504 5. E. J. J. Kalis, L. P. Weng, E. J. M. Temminghoff, W. H. van Riemsdijk, *Anal.*
505 *Chem.*, 79 (2007) 1555.

506 6. S. Noel, M. L. Tercier-Waeber, L. Lin, J. Buffle, O. Guenat, M. Koudelka-Hep,
507 *Electroanalysis*, 18 (2006) 2061.

508 7. N. Parthasarathy, J. Buffle, *Anal. Chim. Acta*, 284 (1994) 649.

509 8. J. Galceran, E. Companys, J. Puy, J. Cecília, J. L. Garcés, *J. Electroanal. Chem.*, 566
510 (2004) 95.

511 9. E. Companys, J. Cecília, G. Codina, J. Puy, J. Galceran, *J. Electroanal. Chem.*, 576
512 (2005) 21.

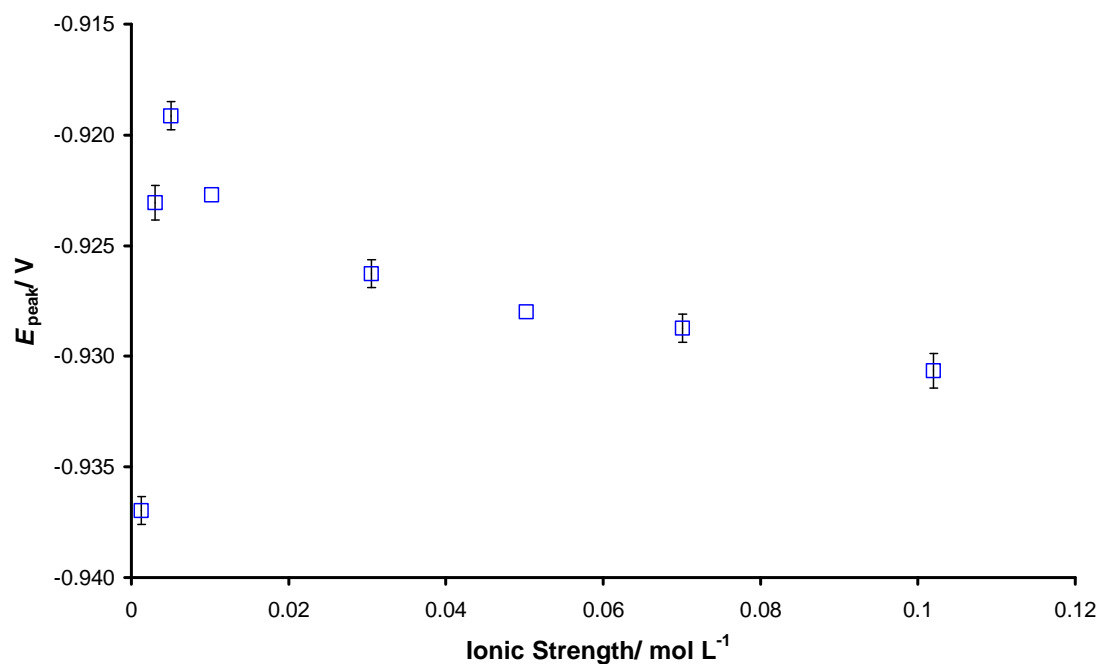
- 513 10. C. Huidobro, E. Companys, J. Puy, J. Galceran, J. P. Pinheiro, J. Electroanal.
514 Chem., 606 (2007) 134.
- 515 11. L. S. Rocha, E. Companys, J. Galceran, H. M. Carapuca, J. P. Pinheiro, Talanta,
516 80 (2010) 1881.
- 517 12. C. Parat, D. Aguilar, L. Authier, M. Potin-Gautier, E. Companys, J. Puy, J.
518 Galceran, Electroanalysis, 23 (2011) 619.
- 519 13. J. Galceran, C. Huidobro, E. Companys, G. Alberti, Talanta, 71 (2007) 1795.
- 520 14. D. Chito, L. Weng, J. Galceran, E. Companys, J. Puy, W. H. van Riemsdijk, H.
521 P. van Leeuwen, Sci. Total Envir., 421-422 (2012) 238.
- 522 15. F. Zavarise, E. Companys, J. Galceran, G. Alberti, A. Profumo, Anal. Bioanal.
523 Chem., 397 (2010) 389.
- 524 16. E. Companys, M. Naval-Sanchez, N. Martinez-Micaelo, J. Puy, J. Galceran, J.
525 Agric. Food Chem., 56 (2008) 8296.
- 526 17. C. David, J. Galceran, C. Rey-Castro, J. Puy, E. Companys, J. Salvador, J.
527 Monné, R. Wallace, A. Vakourov, J. Phys. Chem. C, 116 (2012) 11758.
- 528 18. R. F. Domingos, D. F. Simon, C. Hauser, K. J. Wilkinson, Environ. Sci.
529 Technol., 45 (2011) 7664.
- 530 19. M. Ciszowska, Z. Stojek, J. Electroanal. Chem., 466 (1999) 129.
- 531 20. M. J. Palys, H. Sokolowska, Z. Stojek, Electrochim. Acta., 49 (2004) 3765.
- 532 21. K. B. Oldham, J. C. Myland, Fundamentals of Electrochemical Science,
533 Academic Press, San Diego, 1994.

- 534 22. I. Streeter, R. G. Compton, *J. Phys. Chem. C*, 112 (2008) 13716.
- 535 23. S. M. Silva, A. M. Bond, *Anal. Chim. Acta*, 500 (2003) 307.
- 536 24. O. V. Klymenko, C. Amatore, I. Svir, *Anal. Chem.*, 79 (2007) 6341.
- 537 25. J. Galceran, D. Chito, N. Martinez-Micaelo, E. Companys, C. David, J. Puy, J.
538 *Electroanal. Chem.*, 638 (2010) 131.
- 539 26. C. Parat, L. Authier, D. Aguilar, E. Companys, J. Puy, J. Galceran, M. Potin-
540 Gautier, *Analyst*, 136 (2011) 4337.
- 541 27. M. L. Tercier-Waeber, M. Taillefert, *J. Environ. Monit.*, 10 (2008) 30.
- 542 28. J. D. Allison, D. S. Brown, K. J. Novo-Gradac, U.S. Environmental Protection
543 Agency, Office of Research and Development, Washington, DC.7, 1991.
- 544 29. A. J. Bard, L. R. Faulkner, *Electrochemical Methods. Fundamentals and*
545 *Applications.*, Second edition ed., John Wiley & Sons, Inc., New York, 2001.
- 546 30. F. Berbel, J. M. Díaz-Cruz, C. Ariño, M. Esteban, *J. Electroanal. Chem.*, 475
547 (1999) 99.
- 548 31. R. M. Town, J. P. Pinheiro, R. Domingos, H. P. van Leeuwen, *J. Electroanal.*
549 *Chem.*, 580 (2005) 57.
- 550 32. D. Chito, J. Galceran, E. Companys, *Electroanalysis*, 22 (2010) 2024.
- 551 33. APHA, in L.S.Clesceri, A.E.Greenberg, A.D.Eaton (Eds.), *Standard methods for*
552 *the Examination of water and wastewater*, published jointly by American Public
553 Health Association, American Water Works Association, Water Environment
554 Federation, Washington DC, 1998, Ch.2330B.

555

556

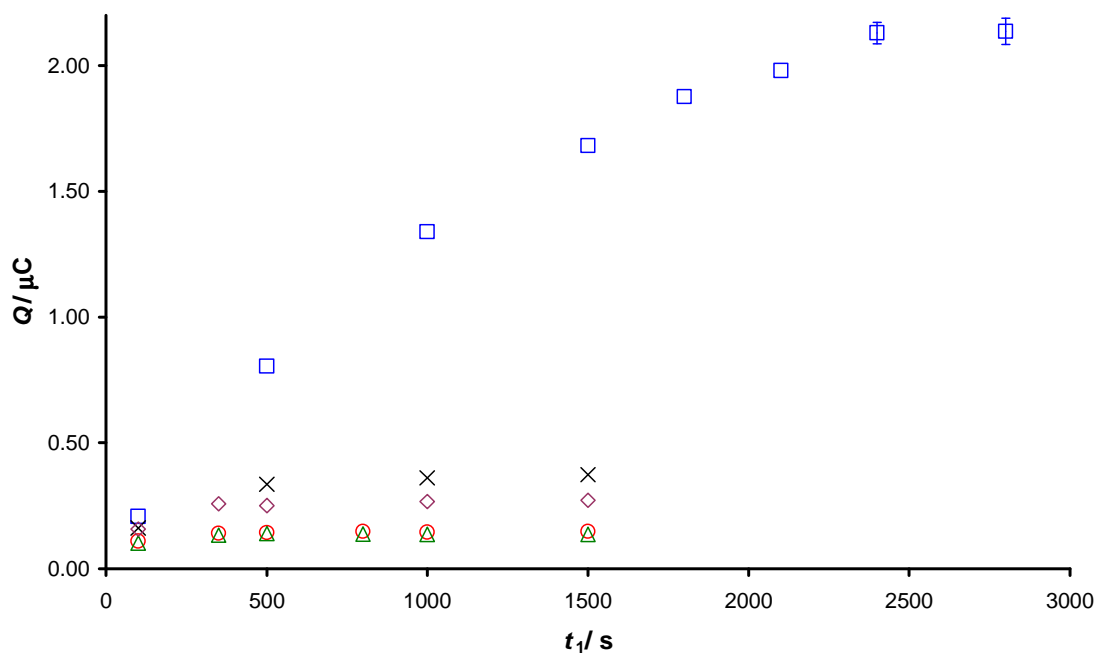
557 **Figures**



558

559 **Figure 1.** Peak potentials from different DPPs performed in a $c_{T,Zn} = 7.5 \times 10^{-6} \text{ mol L}^{-1}$
560 solution with KNO_3 as supporting electrolyte and ionic strengths between 0.001 and 0.1
561 M at $\text{pH}=5.5$. Reference electrode with KNO_3 0.1 mol L^{-1} in the salt bridge. Three
562 different replicates of each measurement have been performed and the standard
563 deviation is shown whenever larger than the marker.

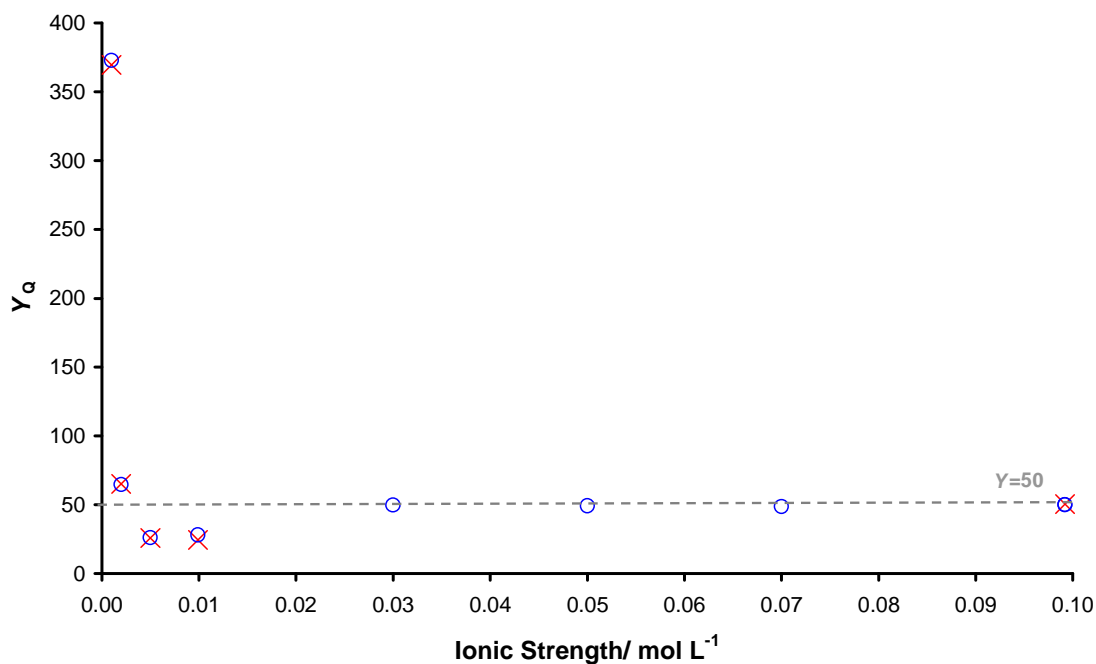
564



565

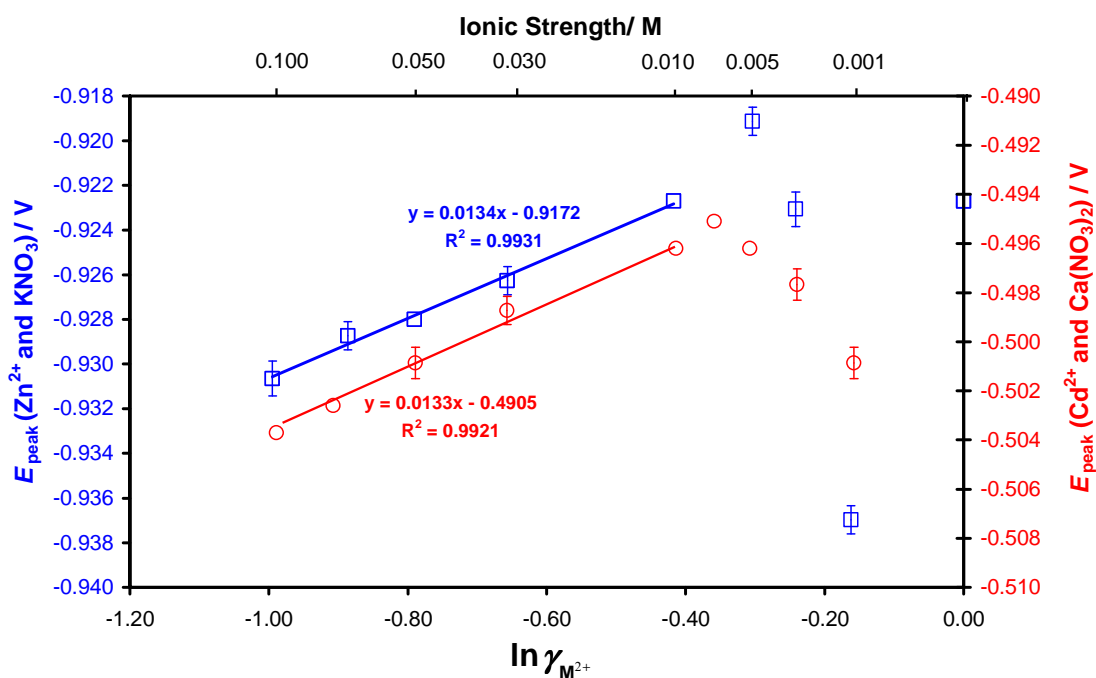
566 **Figure 2.** Trajectories Q vs t_1 for different solutions containing $c_{T,Zn} = 2.5 \times 10^{-6} \text{ mol L}^{-1}$
567 and $\text{KNO}_3 = 0.001(\square)$, $0.002(\times)$, $0.005(\circ)$, $0.01(\Delta)$ and $0.1(\diamond)$ mol L^{-1} at $\text{pH} = 5.5$.
568 AGNES deposition potential has been computed using eqn. (2) with the corresponding
569 E_{peak} at each electrolyte concentration and aiming at $Y=50$ (though the real gain was
570 different, see text). KNO_3 0.1 mol L^{-1} was used as the salt bridge in the reference
571 electrode. Two replicates have been carried out and the standard deviation is shown
572 whenever is larger than the marker.

573

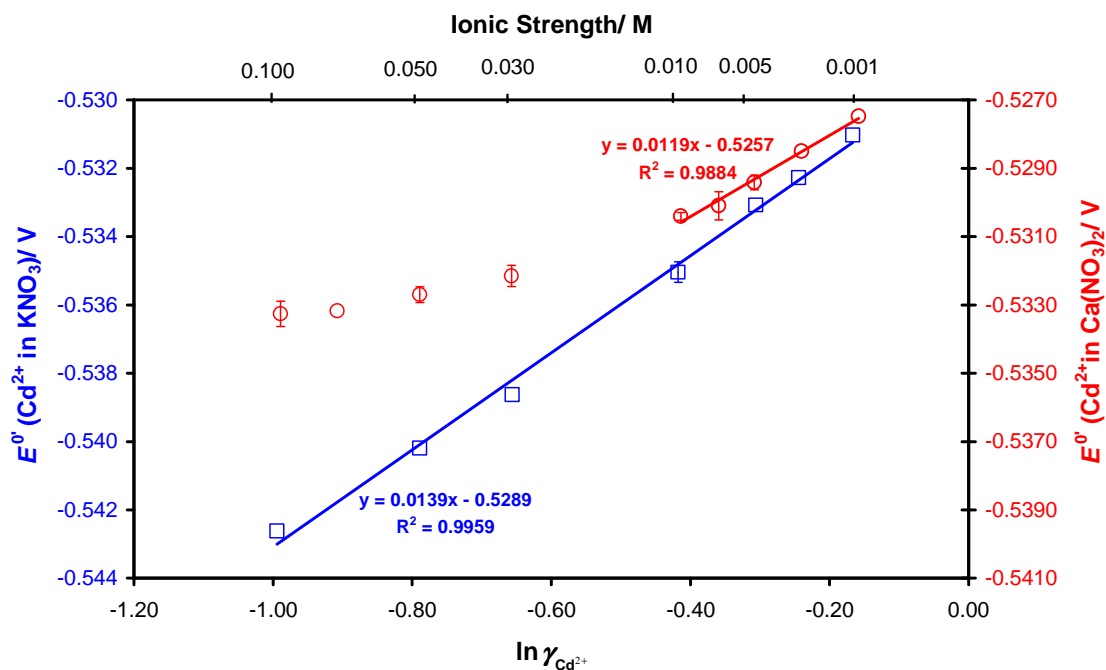


574

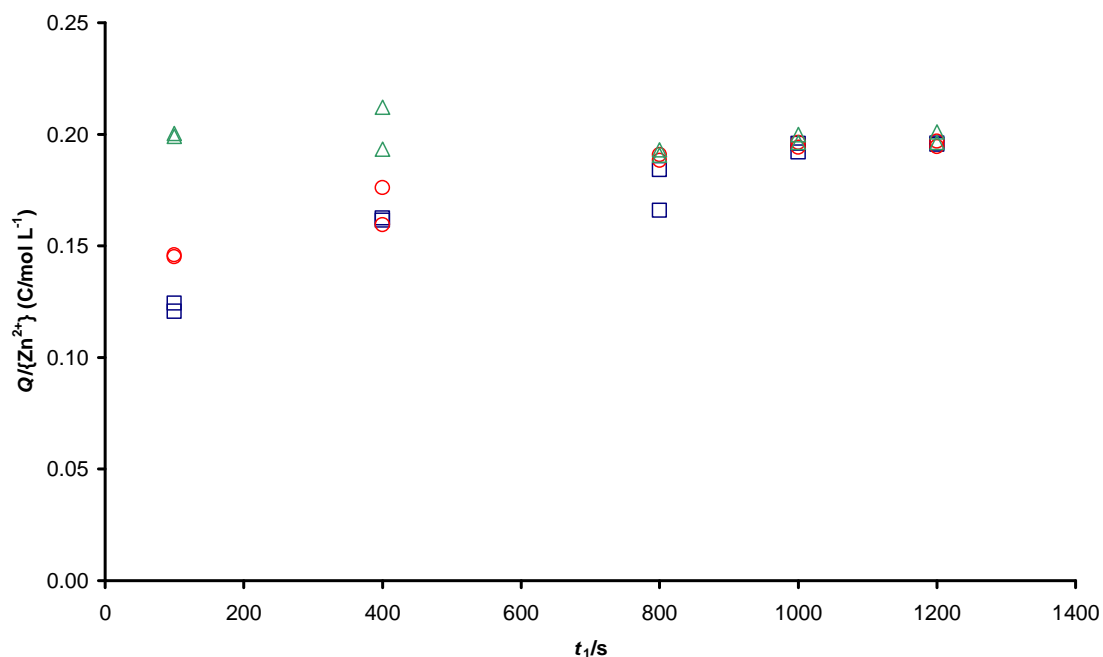
575 **Figure 3.** Comparison between the aimed ($Y=50$, horizontal dash line) and the attained
576 gains (\times , using eqn. (4) and the DPP peaks at the same ionic strength from Figure 1).
577 $c_{T,Zn}=2.5\times 10^{-6}$ mol L $^{-1}$ in KNO $_3$ as supporting electrolyte. The blue circles (\circ) stand for
578 the theoretical gain computed with eqn. (12). Reference electrode with a KNO $_3$ 0.1 mol
579 L $^{-1}$ jacket.



580
581 **Figure 4.** DPP E_{peak} in front of the activity coefficient logarithm in a solution containing
582 $c_{\text{T,Zn}}=7.5\times 10^{-6}$ mol L⁻¹ and KNO₃ as supporting electrolyte (referred to the left hand side
583 axis, \square) or $c_{\text{T,Cd}}=7.5\times 10^{-6}$ and Ca(NO₃)₂ as supporting electrolyte (referred to the right
584 hand side axis, \circ). The ionic strengths studied were between 0.001 and 0.1 mol L⁻¹ (see
585 upper horizontal axis) at pH = 5.5. Reference electrode with salt bridge KNO₃ 0.1 mol
586 L⁻¹ (for KNO₃ background electrolyte) or 1 mol L⁻¹ (for Ca(NO₃)₂ background
587 electrolyte). Three replicates have been carried out and the standard deviation is shown
588 whenever larger than the marker.
589



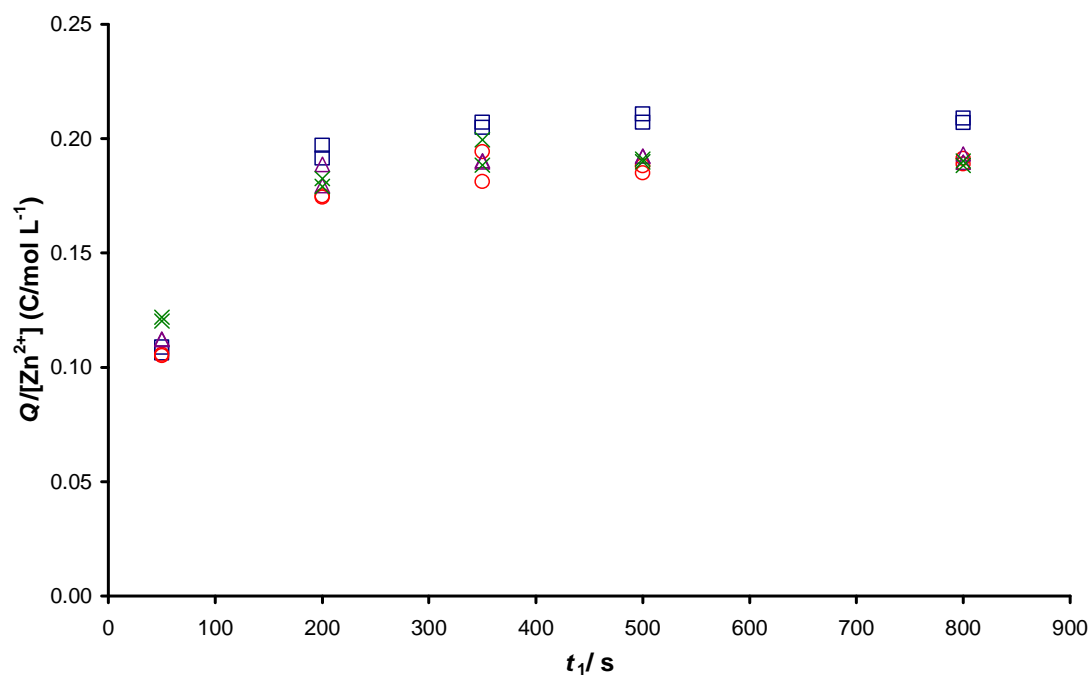
590 **Figure 5.** Representation of $E^{0\prime}$, obtained using eqn. (10) from AGNES experiments, in
 591 front of the activity coefficient logarithm in a solution containing $c_{T,Cd} = 2.5 \times 10^{-6}$ mol
 592 L^{-1} and KNO_3 (referred to the left hand side axis, \square) or $Ca(NO_3)_2$ (referred to the right
 593 hand side axis, \circ) as supporting electrolytes. The ionic strengths were between 0.001
 594 and 0.1 mol L^{-1} at $pH = 5.5$. The deposition potential was $E_1 = -0.5708$ V with a KNO_3
 595 0.1 mol L^{-1} salt bridge in the reference electrode when working with KNO_3 or
 596 $E_1 = -0.5690$ V with a KNO_3 1 mol L^{-1} salt bridge when working with $Ca(NO_3)_2$. Two
 597 replicates have been performed and the standard deviation is shown whenever larger
 598 than the marker.



600

601 **Figure 6.** Trajectories of the quotient $Q/\{Zn^{2+}\}$ vs t_1 for different samples with
602 $c_{T,Zn}=2.5\times 10^{-6}$ M and $[KNO_3]= 0.001(\square)$, $0.01(\circ)$ and $0.1(\Delta)$ mol L⁻¹ showing the
603 collapse of the quotient between retrieved charges and metal activity for sufficiently
604 long times. AGNES has been carried out with a fixed deposition potential ($E_1=-1.0248$
605 V, computed from the DPP of a 0.1 M KNO₃ M sample), KNO₃ 0.1 mol L⁻¹ in the salt
606 bridge and with a fixed $Y=50$ at pH = 5.5. Two different replicates for each experiment
607 have been carried out.

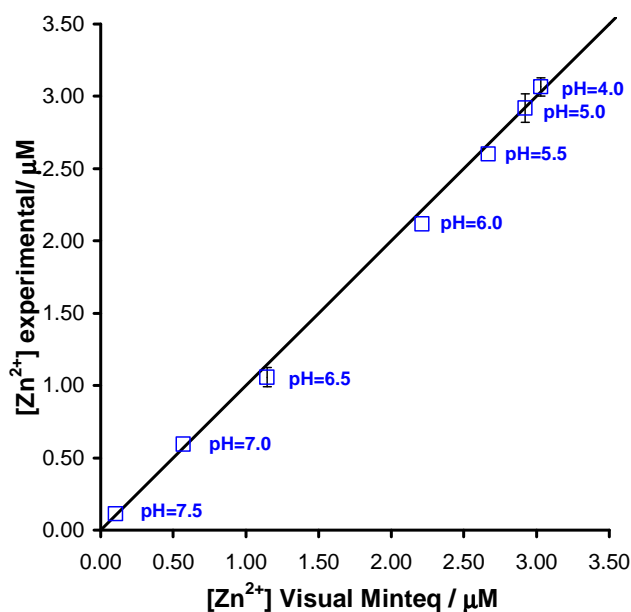
608



609

610 **Figure 7.** Representation of $Q/[Zn^{2+}]$ vs t_1 for solutions with $c_{T,Zn}=2.5 \times 10^{-6} \text{ mol L}^{-1}$ and
611 $\mu=0.001$ (\square), 0.005 (\circ), 0.05 (Δ) and 0.1 (\times) mol L^{-1} at $\text{pH} = 5.5$. AGNES has been
612 performed applying the corresponding deposition potential E_1 , needed to reach $Y=50$,
613 computed with eqn. (12) and using the DPP peak potential of a solution with $\mu=0.1 \text{ mol}$
614 L^{-1} . A reference electrode with a KNO_3 0.1 mol L^{-1} jacket was used. Two different
615 replicates for each experiment have been performed.

616



617

618 **Figure 8.** Free Zn²⁺ concentration, determined with AGNES, in front of the Visual
619 Minteq predicted concentrations at various pHs when a total Zn²⁺ concentration of
620 3.0×10⁻⁶ mol L⁻¹ is complexed with glycine 0.01 M and the ionic strength is 0.001 mol
621 L⁻¹. AGNES was performed with Y₁=50, t₁=350 s, Y₂=10⁻⁸ and Y_{1, sb}=0.01. KNO₃ 0.1 mol
622 L⁻¹ was used as the salt bridge in the reference electrode. Two replicates have been
623 carried out and the standard deviation is shown whenever larger than the marker.

624